

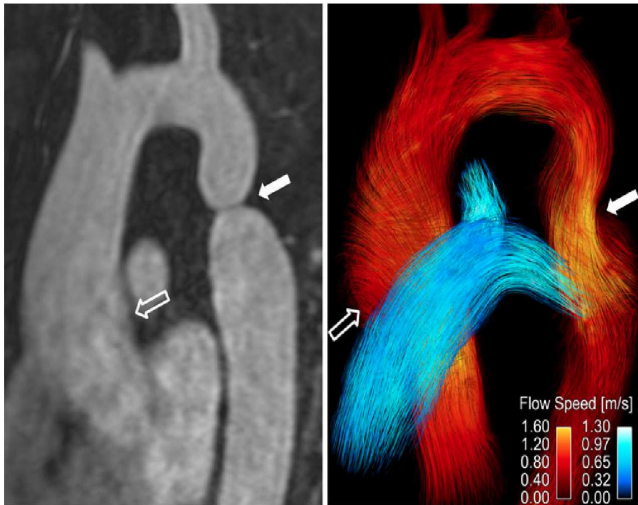
Advances in Quantitative MRI: Acquisition, Estimation, and Application

Gopal Nataraj

Dissertation Defense
March 23, 2018

Dept. of Electrical Engineering and Computer Science
University of Michigan

Example: flow imaging

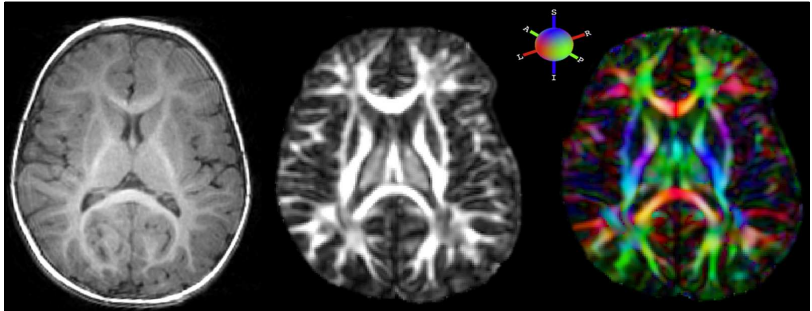


qualitative

quantitative¹

¹figure borrowed from [Hope et al., 2013]

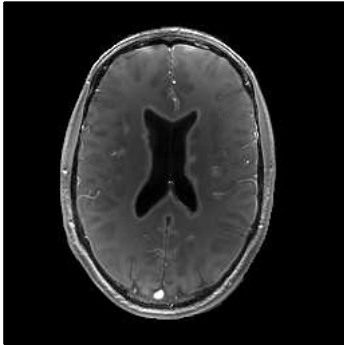
Example: diffusion imaging



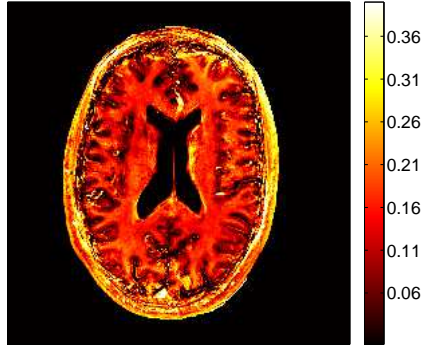
qualitative fractional anisotropy (FA) directional FA²

²figure borrowed from www.diffusion-imaging.com

Example: myelin water imaging



qualitative



fast-relaxing fraction³

³figure adapted from [Nataraj et al., 2017a]

Quantitative MRI (QMRI)

Goal: rapidly and accurately localize biomarkers from MR data

Quantitative MRI (QMRI)

Goal: rapidly and accurately localize biomarkers from MR data

- **biomarker** measurable tissue property (e.g., flow rate)
that indicates a biological process (e.g., blockage)
characteristic to specific disorders (e.g., stroke)

Quantitative MRI (QMRI)

Goal: rapidly and accurately localize biomarkers from MR data

- **biomarker** measurable tissue property (e.g., flow rate)
that indicates a biological process (e.g., blockage)
characteristic to specific disorders (e.g., stroke)
- **localize** produce quantitative MR images

Quantitative MRI (QMRI)

Goal: rapidly and accurately localize biomarkers from MR data

- **biomarker** measurable tissue property (e.g., flow rate)
that indicates a biological process (e.g., blockage)
characteristic to specific disorders (e.g., stroke)
- **localize** produce quantitative MR images
- **accurately** physically realistic signal models
- **rapidly** fast acquisition, fast estimation

Quantitative MRI (QMRI)

Goal: rapidly and accurately localize biomarkers from MR data

- biomarker measurable tissue property (e.g., flow rate)
that indicates a biological process (e.g., blockage)
characteristic to specific disorders (e.g., stroke)
- localize produce quantitative MR images
- accurately physically realistic signal models
- rapidly fast acquisition, fast estimation

Challenge: rapidly vs. accurately often competing goals

- more accurate models typically depend on more markers
- precisely estimating more markers usually requires
longer scans and more computation

Advances in Quantitative MRI:

- **Acquisition**

[Ch. 4]

How can we assemble fast, informative collections of scans to enable precise biomarker quantification?

Advances in Quantitative MRI:

- **Acquisition** [Ch. 4]
How can we assemble fast, informative collections of scans to enable precise biomarker quantification?
- **Estimation** [Ch. 5]
Given accurate models and informative data, how can we rapidly quantify these biomarkers?

Advances in Quantitative MRI:

- **Acquisition** [Ch. 4]
How can we assemble fast, informative collections of scans to enable precise biomarker quantification?
- **Estimation** [Ch. 5]
Given accurate models and informative data, how can we rapidly quantify these biomarkers?
- **Application** [Ch. 6]
Using these tools, can we design a state-of-the-art biomarker?

Advances in Quantitative MRI:

- **Acquisition** [Ch. 4]
How can we assemble fast, informative collections of scans to enable precise biomarker quantification?
- **Estimation** [Ch. 5]
Given accurate models and informative data, how can we rapidly quantify these biomarkers?
- **Application** [Ch. 6]
Using these tools, can we design a state-of-the-art biomarker?

After reconstruction, single voxel y_d in d th image modeled as

$$y_d = s_d(\mathbf{x}; \boldsymbol{\nu}, \mathbf{p}_d) + \epsilon_d \quad (1)$$

- $\mathbf{x} \in \mathbb{R}^L$ unknown parameters
- $\boldsymbol{\nu} \in \mathbb{R}^K$ “known” parameters
- $\mathbf{p}_d \in \mathbb{R}^A$ acquisition parameters
- $s_d : \mathbb{R}^{L+K+A} \mapsto \mathbb{C}$ d th signal model
- $\epsilon_d \in \mathbb{C}$ noise $\sim \mathbb{CN}(0, \sigma_d^2)$

Signal Model

A *scan profile* is a set of D scans that produces at each voxel a measurement vector $\mathbf{y} := [y_1, \dots, y_D]^T$ modeled as

$$\mathbf{y} = \mathbf{s}(\mathbf{x}; \boldsymbol{\nu}, \mathbf{P}) + \boldsymbol{\epsilon} \quad (1)$$

- $\mathbf{x} \in \mathbb{R}^L$ unknown parameters
- $\boldsymbol{\nu} \in \mathbb{R}^K$ “known” parameters
- $\mathbf{P} := [\mathbf{p}_1, \dots, \mathbf{p}_D]$ acquisition parameter matrix
- $\mathbf{s} : \mathbb{R}^{L+K+AD} \mapsto \mathbb{C}^D$ vector signal model
- $\boldsymbol{\epsilon} \sim \mathbb{CN}(\mathbf{0}_D, \boldsymbol{\Sigma})$ noise, with $\boldsymbol{\Sigma} := \text{diag}(\sigma_1^2, \dots, \sigma_D^2)$

Signal Model

A *scan profile* is a set of D scans that produces at each voxel a measurement vector $\mathbf{y} := [y_1, \dots, y_D]^T$ modeled as

$$\mathbf{y} = \mathbf{s}(\mathbf{x}; \boldsymbol{\nu}, \mathbf{P}) + \boldsymbol{\epsilon} \quad (1)$$

- $\mathbf{x} \in \mathbb{R}^L$ unknown parameters
- $\boldsymbol{\nu} \in \mathbb{R}^K$ “known” parameters
- $\mathbf{P} := [\mathbf{p}_1, \dots, \mathbf{p}_D]$ acquisition parameter matrix
- $\mathbf{s} : \mathbb{R}^{L+K+AD} \mapsto \mathbb{C}^D$ vector signal model
- $\boldsymbol{\epsilon} \sim \mathbb{CN}(\mathbf{0}_D, \boldsymbol{\Sigma})$ noise, with $\boldsymbol{\Sigma} := \text{diag}(\sigma_1^2, \dots, \sigma_D^2)$

Task: design \mathbf{P} to enable precise unbiased estimation of \mathbf{x}

Towards an Objective Function

When \mathbf{s} is analytic in \mathbf{x} (as is typical),

Fisher information characterizes unbiased estimator precision:

$$\mathbf{F}(\mathbf{x}; \boldsymbol{\nu}, \mathbf{P}) := (\nabla_{\mathbf{x}} \mathbf{s}(\mathbf{x}; \boldsymbol{\nu}, \mathbf{P}))^H \boldsymbol{\Sigma}^{-1} \nabla_{\mathbf{x}} \mathbf{s}(\mathbf{x}; \boldsymbol{\nu}, \mathbf{P}). \quad (2)$$

Towards an Objective Function

When \mathbf{s} is analytic in \mathbf{x} (as is typical),

Fisher information characterizes unbiased estimator precision:

$$\mathbf{F}(\mathbf{x}; \boldsymbol{\nu}, \mathbf{P}) := (\nabla_{\mathbf{x}} \mathbf{s}(\mathbf{x}; \boldsymbol{\nu}, \mathbf{P}))^H \boldsymbol{\Sigma}^{-1} \nabla_{\mathbf{x}} \mathbf{s}(\mathbf{x}; \boldsymbol{\nu}, \mathbf{P}). \quad (2)$$

When \mathbf{F} is invertible, Cramér-Rao Bound (CRB) [Cramér, 1946] ensures covariance of unbiased estimates $\hat{\mathbf{x}}$ of \mathbf{x} satisfy

$$\text{cov } \hat{\mathbf{x}}; \boldsymbol{\nu}, \mathbf{P} \succeq \mathbf{F}^{-1}(\mathbf{x}; \boldsymbol{\nu}, \mathbf{P}). \quad (3)$$

Maximum-likelihood (ML) estimates achieve CRB asymptotically or (equivalently for Gaussian data) at sufficiently high SNR.

Towards an Objective Function

When \mathbf{s} is analytic in \mathbf{x} (as is typical),

Fisher information characterizes unbiased estimator precision:

$$\mathbf{F}(\mathbf{x}; \boldsymbol{\nu}, \mathbf{P}) := (\nabla_{\mathbf{x}} \mathbf{s}(\mathbf{x}; \boldsymbol{\nu}, \mathbf{P}))^H \boldsymbol{\Sigma}^{-1} \nabla_{\mathbf{x}} \mathbf{s}(\mathbf{x}; \boldsymbol{\nu}, \mathbf{P}). \quad (2)$$

When \mathbf{F} is invertible, Cramér-Rao Bound (CRB) [Cramér, 1946] ensures covariance of unbiased estimates $\hat{\mathbf{x}}$ of \mathbf{x} satisfy

$$\text{cov } \hat{\mathbf{x}}; \boldsymbol{\nu}, \mathbf{P} \succeq \mathbf{F}^{-1}(\mathbf{x}; \boldsymbol{\nu}, \mathbf{P}). \quad (3)$$

Maximum-likelihood (ML) estimates achieve CRB asymptotically or (equivalently for Gaussian data) at sufficiently high SNR.

Idea: choose \mathbf{P} such that imprecision matrix \mathbf{F}^{-1} “small”

Idea: choose \mathbf{P} to minimize the objective

$$\Psi(\mathbf{x}; \nu, \mathbf{P}) = \text{tr}\left(\mathbf{W}\mathbf{F}^{-1}(\mathbf{x}; \nu, \mathbf{P})\mathbf{W}^T\right), \quad (4)$$

where $\mathbf{W} \in \mathbb{R}^{L \times L}$ is a pre-selected diagonal matrix of weights.

Idea: choose \mathbf{P} to minimize the objective

$$\Psi(\mathbf{x}; \nu, \mathbf{P}) = \text{tr}\left(\mathbf{W}\mathbf{F}^{-1}(\mathbf{x}; \nu, \mathbf{P})\mathbf{W}^T\right), \quad (4)$$

where $\mathbf{W} \in \mathbb{R}^{L \times L}$ is a pre-selected diagonal matrix of weights.

Challenge: \mathbf{x}, ν vary spatially

Idea: choose \mathbf{P} to minimize the objective

$$\Psi(\mathbf{x}; \boldsymbol{\nu}, \mathbf{P}) = \text{tr}(\mathbf{W}\mathbf{F}^{-1}(\mathbf{x}; \boldsymbol{\nu}, \mathbf{P})\mathbf{W}^T), \quad (4)$$

where $\mathbf{W} \in \mathbb{R}^{L \times L}$ is a pre-selected diagonal matrix of weights.

Challenge: $\mathbf{x}, \boldsymbol{\nu}$ vary spatially

Two problems considered:

- min-max scan design [Nataraj et al., 2017b]

$$\check{\mathbf{P}} \in \left\{ \arg \min_{\mathbf{P} \in \mathbb{P}} \max_{\substack{\mathbf{x} \in \mathbb{X}^t \\ \boldsymbol{\nu} \in \mathbb{N}^t}} \Psi(\mathbf{x}; \boldsymbol{\nu}, \mathbf{P}) \right\} \quad (5)$$

where $\mathbb{X}^t \subseteq \mathbb{R}^L$ and $\mathbb{N}^t \subseteq \mathbb{R}^K$ are “tight” ranges of interest and \mathbb{P} is defined by acquisition/timing constraints

Idea: choose \mathbf{P} to minimize the objective

$$\Psi(\mathbf{x}; \boldsymbol{\nu}, \mathbf{P}) = \text{tr}(\mathbf{W}\mathbf{F}^{-1}(\mathbf{x}; \boldsymbol{\nu}, \mathbf{P})\mathbf{W}^T), \quad (4)$$

where $\mathbf{W} \in \mathbb{R}^{L \times L}$ is a pre-selected diagonal matrix of weights.

Challenge: $\mathbf{x}, \boldsymbol{\nu}$ vary spatially

Two problems considered:

- min-max scan design [Nataraj et al., 2017b]

$$\check{\mathbf{P}} \in \left\{ \arg \min_{\mathbf{P} \in \mathbb{P}} \max_{\substack{\mathbf{x} \in \mathbb{X}^t \\ \boldsymbol{\nu} \in \mathbb{N}^t}} \Psi(\mathbf{x}; \boldsymbol{\nu}, \mathbf{P}) \right\} \quad (5)$$

- Bayesian scan design

$$\check{\mathbf{P}} \in \left\{ \arg \min_{\mathbf{P} \in \mathbb{P}} E_{\mathbf{x}, \boldsymbol{\nu}}(\Psi(\mathbf{x}; \boldsymbol{\nu}, \mathbf{P})) \right\} \quad (6)$$

Scan Design

Idea: choose \mathbf{P} to minimize the objective

$$\Psi(\mathbf{x}; \boldsymbol{\nu}, \mathbf{P}) = \text{tr}(\mathbf{W}\mathbf{F}^{-1}(\mathbf{x}; \boldsymbol{\nu}, \mathbf{P})\mathbf{W}^T), \quad (4)$$

where $\mathbf{W} \in \mathbb{R}^{L \times L}$ is a pre-selected diagonal matrix of weights.

Challenge: $\mathbf{x}, \boldsymbol{\nu}$ vary spatially

Two problems considered:

- min-max scan design [Nataraj et al., 2017b]

$$\check{\mathbf{P}} \in \left\{ \arg \min_{\mathbf{P} \in \mathbb{P}} \max_{\substack{\mathbf{x} \in \mathbb{X}^t \\ \boldsymbol{\nu} \in \mathbb{N}^t}} \Psi(\mathbf{x}; \boldsymbol{\nu}, \mathbf{P}) \right\} \quad (5)$$

- Bayesian scan design

$$\check{\mathbf{P}} \in \left\{ \arg \min_{\mathbf{P} \in \mathbb{P}} E_{\mathbf{x}, \boldsymbol{\nu}}(\Psi(\mathbf{x}; \boldsymbol{\nu}, \mathbf{P})) \right\} \quad (6)$$

Detailed Example Study

Task: design fast acquisition for precise estimation of relaxation parameters T_1 , T_2 in white/gray matter (WM/GM) of brain

Detailed Example Study

Task: design fast acquisition for precise estimation of relaxation parameters T_1 , T_2 in white/gray matter (WM/GM) of brain

- Consider scan profiles consisting of two fast pulse sequences
 - Spoiled Gradient-Recalled Echo (SPGR) [Zur et al., 1991]
 - Dual-Echo Steady-State (DESS) [Redpath and Jones, 1988]

Detailed Example Study

Task: design fast acquisition for precise estimation of relaxation parameters T_1, T_2 in white/gray matter (WM/GM) of brain

- Consider scan profiles consisting of two fast pulse sequences
 - Spoiled Gradient-Recalled Echo (SPGR) [Zur et al., 1991]
 - Dual-Echo Steady-State (DESS) [Redpath and Jones, 1988]
- For each scan profile feasible under total time constraint:
 1. Let \mathbf{s} model corresponding single-component signal
 - $\mathbf{x} \leftarrow [m_0, T_1, T_2]^T$, where m_0 is a scale factor
 - $\nu \leftarrow$ flip angle variation
 - $\mathbf{P} \leftarrow$ nominal flip angles, repetition times
 2. Optimize \mathbf{P} subject to flip angle, sequence timing constraints
 - $\mathbf{W} \leftarrow \text{diag}(0, 0.1, 1)$ emphasizes T_1, T_2 est roughly equally
 - \mathbb{X}^t chosen to focus on WM/GM at 3T field strength
 - \mathbb{N}^t chosen to allow 10% flip angle variation

Scan Profile Comparison

(#SPGR, #DESS) Profiles	(2, 1)	(1, 1)	(0, 2)
SPGR nom. flip (deg)	(15, 5)	15	–
DESS nom. flip (deg)	30	10	(35, 10)
SPGR rep. times (ms)	(12.2, 12.2)	13.9	–
DESS rep. times (ms)	17.5	28.0	(24.4, 17.5)
optimal max cost	4.0	4.9	3.5

Scan Profile Comparison

(#SPGR, #DESS) Profiles	(2, 1)	(1, 1)	(0, 2)
SPGR nom. flip (deg)	(15, 5)	15	–
DESS nom. flip (deg)	30	10	(35, 10)
SPGR rep. times (ms)	(12.2, 12.2)	13.9	–
DESS rep. times (ms)	17.5	28.0	(24.4, 17.5)
optimal max cost	4.0	4.9	3.5

Main finding: 2 DESS sequences can yield T_1 , T_2 WM/GM estimates that are at least as precise as T_1 , T_2 estimates from SPGR/DESS scan profiles, under this competitive time constraint.

Experimental Setup

Candidate $(2, 1)$, $(1, 1)$, $(0, 2)$ SPGR/DESS scan profiles

- Prescribed optimized nominal flip angles, repetition times
- Used $256 \times 256 \times 8$ 3D matrix over $24 \times 24 \times 4$ cm FOV
- Required **1m37s** scan time for each profile

Experimental Setup

Candidate (2, 1), (1, 1), (0, 2) SPGR/DESS scan profiles

- Prescribed optimized nominal flip angles, repetition times
- Used $256 \times 256 \times 8$ 3D matrix over $24 \times 24 \times 4$ cm FOV
- Required **1m37s** scan time for each profile

Reference scan profile

- Four inversion recovery (IR) scans for T_1 estimation
- Four spin-echo (SE) scans for T_2 estimation
- 256×256 matrix over $24 \times 24 \times 0.5$ cm FOV
- Required **40m58s** scan time total

Experimental Setup

Candidate (2, 1), (1, 1), (0, 2) SPGR/DESS scan profiles

- Prescribed optimized nominal flip angles, repetition times
- Used $256 \times 256 \times 8$ 3D matrix over $24 \times 24 \times 4$ cm FOV
- Required **1m37s** scan time for each profile

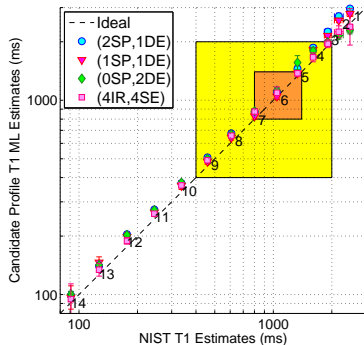
Reference scan profile

- Four inversion recovery (IR) scans for T_1 estimation
- Four spin-echo (SE) scans for T_2 estimation
- 256×256 matrix over $24 \times 24 \times 0.5$ cm FOV
- Required **40m58s** scan time total

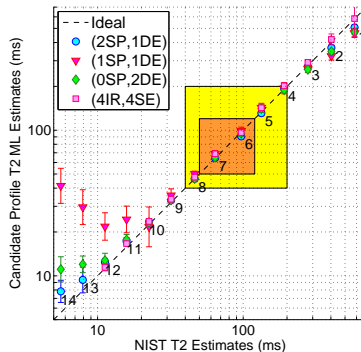
Bloch-Siegert (BS) acquisition for separate flip angle calibration

- Acquired 2 BS-shifted 3D SPGR scans in 1m40s total
- Used for T_1 , T_2 est from both candidate and reference profiles

Phantom Accuracy Results



(a) \hat{T}_1^{ML} Estimates



(b) \hat{T}_2^{ML} Estimates

Compared against NIST NMR measurements [Keenan et al., 2016]

Phantom Precision Results

- Repeated each profile 10 times
- Estimated T_1 , T_2 std dev of typical voxel across repetitions

Phantom Precision Results

	(2, 1)	(1, 1)	(0, 2)
V5 $\hat{\sigma}_{\hat{T}_1^{\text{ML}}}$	50 ± 12	$40 \pm 10.$	39 ± 9.4
V6 $\hat{\sigma}_{\hat{T}_1^{\text{ML}}}$	70 ± 18	60 ± 15	60 ± 16
V7 $\hat{\sigma}_{\hat{T}_1^{\text{ML}}}$	60 ± 13	50 ± 13	50 ± 13
V5 $\hat{\sigma}_{\hat{T}_2^{\text{ML}}}$	2.6 ± 0.63	6 ± 1.4	3.5 ± 0.84
V6 $\hat{\sigma}_{\hat{T}_2^{\text{ML}}}$	1.9 ± 0.46	5 ± 1.1	2.3 ± 0.54
V7 $\hat{\sigma}_{\hat{T}_2^{\text{ML}}}$	1.4 ± 0.34	3.4 ± 0.80	1.5 ± 0.35
$\sqrt{\text{opt max cost}}$ estimate	8.9 ± 1.8	11 ± 2.6	8.3 ± 2.1

Table 1: Pooled sample standard deviations \pm pooled standard errors of sample standard deviations (ms), from optimized SPGR/DESS profiles.

Phantom Precision Results

	(2, 1)	(1, 1)	(0, 2)
V5 $\hat{\sigma}_{\hat{T}_1^{\text{ML}}}$	50 ± 12	$40 \pm 10.$	39 ± 9.4
V6 $\hat{\sigma}_{\hat{T}_1^{\text{ML}}}$	70 ± 18	60 ± 15	60 ± 16
V7 $\hat{\sigma}_{\hat{T}_1^{\text{ML}}}$	60 ± 13	50 ± 13	50 ± 13
V5 $\hat{\sigma}_{\hat{T}_2^{\text{ML}}}$	2.6 ± 0.63	6 ± 1.4	3.5 ± 0.84
V6 $\hat{\sigma}_{\hat{T}_2^{\text{ML}}}$	1.9 ± 0.46	5 ± 1.1	2.3 ± 0.54
V7 $\hat{\sigma}_{\hat{T}_2^{\text{ML}}}$	1.4 ± 0.34	3.4 ± 0.80	1.5 ± 0.35
$\sqrt{\text{opt max cost}}$ estimate	8.9 ± 1.8	11 ± 2.6	8.3 ± 2.1

Table 1: Pooled sample standard deviations \pm pooled standard errors of sample standard deviations (ms), from optimized SPGR/DESS profiles.

Similar trends across profiles of empirical vs. theoretical std dev!

Contributions

- MR scan design method for precise parameter estimation
- Fast SPGR/DESS scan profile for T_1 , T_2 estimation in brain

Contributions

- MR scan design method for precise parameter estimation
- Fast SPGR/DESS scan profile for T_1 , T_2 estimation in brain
 - Phantom (and omitted simulation) results validate method as a predictor of unbiased estimation precision.

Summary

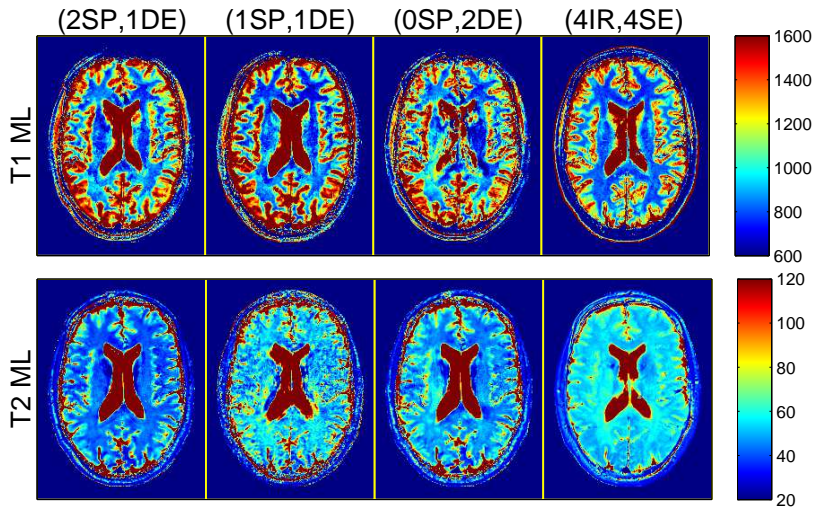


Figure 1: Colorbar ranges in ms.

Contributions

- MR scan design method for precise parameter estimation
- Fast SPGR/DESS scan profile for T_1 , T_2 estimation in brain
 - Phantom (and omitted simulation) results validate method as a predictor of unbiased estimation precision.
 - *In vivo* results reveal discrepancies (especially in T_2 estimates), suggesting T_1 , T_2 estimates sensitive to model mismatch.

Contributions

- MR scan design method for precise parameter estimation
- Fast SPGR/DESS scan profile for T_1 , T_2 estimation in brain
 - Phantom (and omitted simulation) results validate method as a predictor of unbiased estimation precision.
 - *In vivo* results reveal discrepancies (especially in T_2 estimates), suggesting T_1 , T_2 estimates sensitive to model mismatch.

How to address *in vivo* model mismatch?

- More accurate *in vivo* signal models
- More scalable parameter estimation

Advances in Quantitative MRI:

- **Acquisition** [Ch. 4]
How can we assemble fast, informative collections of scans to enable precise biomarker quantification?
- **Estimation** [Ch. 5]
Given accurate models and informative data, how can we rapidly quantify these biomarkers?
- **Application** [Ch. 6]
Using these tools, can we design a state-of-the-art biomarker?

Advances in Quantitative MRI:

- **Acquisition** [Ch. 4]
How can we assemble fast, informative collections of scans to enable precise biomarker quantification?
- **Estimation** [Ch. 5]
Given accurate models and informative data, how can we rapidly quantify these biomarkers?
- **Application** [Ch. 6]
Using these tools, can we design a state-of-the-art biomarker?



Cramér, H. (1946).

Mathematical methods of statistics.

Princeton Univ. Press, Princeton.



Hope, M. D., Wrenn, S. J., and Dyverfeldt, P. (2013).

Clinical applications of aortic 4d flow imaging.

Curr. Cardiovasc. Imag. Rep., 6(2):128–39.



Keenan, K. E., Stupic, K. F., Boss, M. A., Russek, S. E., Chenevert, T. L., Prasad, P. V., Reddick, W. E., Cecil, K. M., Zheng, J., Hu, P., and Jackson, E. F. (2016).

Multi-site, multi-vendor comparison of T1 measurement using ISMRM/NIST system phantom.

In *Proc. Intl. Soc. Mag. Res. Med.*, page 3290.



Nataraj, G., Nielsen, J.-F., and Fessler, J. A. (2017a).
Myelin water fraction estimation from optimized steady-state sequences using kernel ridge regression.
In Proc. Intl. Soc. Mag. Res. Med., page 5076.



Nataraj, G., Nielsen, J.-F., and Fessler, J. A. (2017b).
Optimizing MR scan design for model-based T1, T2 estimation from steady-state sequences.
IEEE Trans. Med. Imag., 36(2):467–77.



Redpath, T. W. and Jones, R. A. (1988).
FADE-A new fast imaging sequence.
Mag. Res. Med., 6(2):224–34.



Zur, Y., Wood, M. L., and Neuringer, L. J. (1991).
Spoiling of transverse magnetization in steady-state sequences.
Mag. Res. Med., 21(2):251–63.